Journal of AppliedMath 2024, 2(3), 1437.
https://doi.org/10.59400/jam.v2i3.1437

Article

Parameter estimation for photovoltaic systems: An enhanced Broyden-like approach

Isaac Azure[1,*], Stephen B. Twum[2], Baba Seidu[2]

[1] Mathematics Department, University for Development Studies, Tamale P. O. Box TL1350, Ghana
[2] Mathematics Department, C.K. Tedam University of Technology and Applied Sciences, Navrongo CKT-UTAS Box 24, Ghana
*** Corresponding author:** Azure Isaac, azureike@yahoo.com

CITATION

Azure I, Twum SB, Seidu B. Parameter estimation for photovoltaic systems: An enhanced Broyden-like approach. Journal of AppliedMath. 2024; 2(3): 1437. https://doi.org/10.59400/jam.v2i3.1437

ARTICLE INFO

Received: 6 June 2024
Accepted: 1 July 2024
Available online: 1 August 2024

Abstract: Solar energy, specifically photovoltaic systems, has emerged as a prevalent source of electrical power worldwide, gaining acceptance on many continents. While numerous African countries are gradually embracing this alternative energy due to abundant sunlight, the high cost of solar panels and accessories remains a barrier to widespread adoption. This study focuses on refining recently developed iterative methods, leveraging quadrature rules of integration, to accurately estimate parameters in the design of photovoltaic (PV) systems for predetermined power outputs under diverse environmental conditions. The research compares these methods, particularly the authors' MS-3/8 and TS-3/8 approaches, with the commonly used Newton-Raphson method. In the examination, a 10 W PV system with a single diode PV module is considered. Results indicate that the MS-3/8 method demonstrates greater efficiency and requires fewer iterations to converge to the estimated power output of the PV system compared to the Newton-Raphson method and other approaches by different authors. Ultimately, the research introduces a suggested mathematical model for a Four-Diode PV system, offering an alternative method for determining the parameters of the photovoltaic system.

Keywords: photovoltaic system; solar energy; quadrature rules; single diode; power output; mathematical model; current; voltage

1. Introduction

Background

Solar energy stands out as the most abundant renewable resource globally, facilitated by solar rays—electromagnetic waves delivering essential light and heat to sustain terrestrial life. Upon reaching the Earth's surface as solar irradiation, this energy undergoes transformation into electrical energy. Two primary power plants enable this conversion: (i) photovoltaic (PV) systems, comprising arrays of semiconductor-based modules like silicon and germanium, directly converting solar irradiation into electricity; and (ii) heliothermic systems, generating electricity through fluid heating, functioning akin to traditional thermoelectric generators [1].

The PV system has proven superior, rendering it more competitive among various power sources. Its effectiveness hinges on three key factors: the PV module's efficiency, determined by construction methods, materials, and converter design; the maximum power point tracking (MPPT) algorithm's efficiency, controlling the system's optimal power point; and the efficiency of the maximum power point tracking (MPPT) [2]. Enhancing PV module and converter efficiency involves labor-intensive manufacturer research and development, while improving the MPPT

algorithm is a simpler and cost-effective endeavor [2].

Manufacturers typically construct and evaluate PV modules under standard test conditions (STC) with solar radiation at 1000 W/m^2, cell temperature at 25 ℃, and a solar spectrum of 1.5. The parameters crucial for PV module input are subject to the area's meteorological conditions, introducing unpredictability due to the random nature of climatic occurrences [3]. These uncertainties within the PV system contribute to overestimations or underestimations of PV module energy yield. To establish and refine control algorithms, extracting PV module parameters becomes imperative, serving as the cornerstone for determining energy yield.

Notably, solar panel specifications have been previously extracted by researchers at the Centre for Research and Extension in Alternative Energies (NUPEA) [4].

This study aims to extract PV system parameters using recently developed methods by the authors [1,3,5], for the numerical solution of systems of nonlinear equations, which arise from the mathematical modeling of PV systems. A comparative analysis is conducted between the results of the study by Isaac et al. [1,3], which utilized the Newton-Raphson method for estimating PV system parameters, and the results obtained by the authors using the same secondary dataset. Subsequently, primary datasets collected by the authors are employed for parameter estimation, and the results are thoroughly analyzed. In summary, this study had three main objectives:

1) Conduct a comparative analysis between the Newton-Raphson method and the MS-3/8 and TS-3/8 methods, utilizing secondary data from a 40 W PV module.
2) Employ the MS-3/8 and TS-3/8 methods to estimate the parameters of a 10 W PV module and assess their applicability for determining its specific parameters.
3) Introduce a mathematical model for a four-diode PV module, presenting a novel approach to describing and understanding its characteristics and behavior in photovoltaic systems.

2. Literature review

A solar cell, also known as a photovoltaic (PV) cell, is fundamentally a p-n junction created in a thin semiconductor wafer or layer. Utilizing the photovoltaic effect, the electromagnetic radiation from solar energy can be directly converted into electricity [6]. Photons possessing energy greater than the semiconductor's band-gap energy are absorbed, leading to the creation of an electron-hole pair in proportion to the incident irradiation. In a simplified explanation of the PV system's operation, internal electric fields within the p-n junction segregate these carriers, resulting in a photo-current that is directly proportional to the solar irradiation.

To construct a circuit that accurately mimics a photovoltaic (PV) cell, one must first grasp its physical structure and the electrical characteristics of its components. The ideal equivalent electrical circuit for a PV cell involves a current source in series with a single-diode PV cell [7,8]. **Figure 1** illustrates the electrical circuit configuration of a single-diode solar cell.

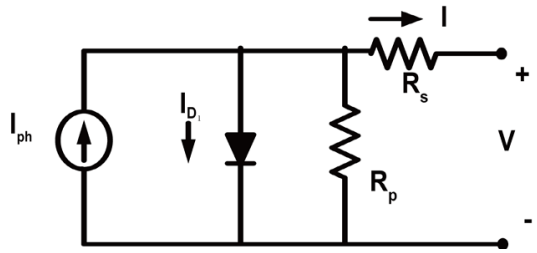

Figure 1. Electrical circuit of PV cell with single-diode [9].

Among various options, the single-diode PV module stands out as the most popular and widely employed. In the modeling of PV systems, it serves as the simplest module utilized by many authors when extracting parameters related to the PV system. Under known temperature and irradiance conditions, the cell's parameters are determined at three key operating points: open circuit, short circuit, and maximum power. The output current equation for the circuit depicted in **Figure 1** is provided as follows:

$$I = I_{\mathrm{PV}} - I_D \tag{1}$$

where,

$$I_D = I_0 \left[\exp\left(\frac{v}{AV_T}\right) - 1\right], \tag{2}$$

Substituting Equation (2) into Equation (1), the main output current equation, becomes:

$$I = I_{\mathrm{PV}} - I_0 \left[\exp\left(\frac{v}{AV_T}\right) - 1\right], \tag{3}$$

where, I_{PV} is the current generated by the incidence of light; I_0 is the diode reverse bias saturation current; V_T is the thermal voltage of the PV module having N_S cells connected in series; q is the electron charge; K is the Boltzmann constant; T is the temperature of the p-n junction and A is the diode ideality factor. V_T is expressed as:

$$V_T = \frac{N_S K T}{q} \tag{4}$$

PV cells are defined by the short circuit current (I_{sc}), open circuit voltage (V_{oc}), or ideality factor (A), which are the three primary operating points in a PV system simulation. A current source's output is proportional to the amount of light falling on the cell. The short circuit current (I_{sc}) is the highest value of the current generated by the cell under the same irradiance and p-n junction temperature circumstances [8,9].

The short circuit current is calculated at $V = 0$, yielding from Equation (3):

$$I_{sc} = I = I_{\mathrm{PV}} \tag{5}$$

The open circuit voltage (V_{oc}) is the highest value of the voltage at the cell terminals under the same irradiance and temperature conditions, and it may be represented as:

$$V = V_{oc} = AV_T \ln\left[1 + \frac{I_{sc}}{I_0}\right], I = 0 \tag{6}$$

Thus, at the same conditions used for short circuit current and open circuit voltage, the power output of an ideal (single-diode) PV cell is given as:

$$P = V\left\{I_{\mathrm{PV}} - I_0 \left[\exp\left(\frac{v}{AV_T}\right) - 1\right]\right\} \tag{7}$$

Similar to the single-diode module, the double-diode module introduces an additional diode (diode quality factor) to the photovoltaic (PV) cell, thereby augmenting the number of parameters within the cell. Some authors suggest that this extra diode significantly alters the outcomes of the double-diode PV cell, providing more accurate results compared to the single-diode PV cell [10].

In contrast to the single-diode and double-diode PV cells, the three-diode module incorporates three diodes, resulting in a total of nine unknown parameters in the module. Research by Benabdelkrim and Benatillah [11], Kisabo et al. [12] demonstrates the advantages of the three-diode PV module in extracting parameters for PV systems. When compared to the single- and double-diode models, the three-diode model proves to be more efficient in acquiring PV system data [12]. Existing literature implies a trend that suggests that the more diodes present, the more efficient the module becomes.

The succeeding section delves into the mathematical modeling of a PV system and provides a brief discussion of the methods employed for parameter determination. This is followed by the results and discussions section and, finally, the concluding section.

3. Mathematical model of a PV system

Mathematical models can be constructed to facilitate the extraction of parameters for photovoltaic (PV) systems, focusing on the PV cell as the fundamental unit. This section is dedicated to the modeling of a single-diode PV system, treating it as a system of nonlinear equations based on its specific configuration.

For engineers seeking a quick reference to assess the performance of a PV system, the experimental current (I) and voltage (V) characteristics parameters of the Solarex MSX60, a single-diode module, are extracted. The obtained results are expected to align with the manufacturer's provided experimental data, confirming the suitability of the presented module [13].

Various circuit modules have been devised to characterize the properties of photovoltaic systems, with single- and double-diode modules being the most widely employed. In certain instances, characteristics such as leakage or reverse saturation current, light-generated current, diode quality factor, shunt resistance, and series resistance can be utilized to encompass a PV cell's full features within a single-diode module. External influences like light-generated current and reverse saturation current, along with internal influences like diode quality factor, shunt resistance, and series resistance, contribute to the comprehensive characterization of a PV cell. Accurate computation of these internal influences is pivotal for ensuring the quality of PV system modeling [11,14].

3.1. Model formulation for single diode PV module

The development of the model employs Kirchhoff's rule [15] for the single-diode PV module, which involves determining five unknown parameters: light-generated current, leakage or reverse saturation current, diode quality factor, series resistance, and shunt resistance [12].

Applying Kirchhoff's current law to the circuit in **Figure 1** gives:

$$I = I_{ph} - I_D - I_{sh} \tag{8}$$

but

$$I_D = I_o \left[\exp\left(\frac{V + IR_s}{AV_T}\right) - 1\right] \tag{9}$$

$$I_{sh} = \frac{V + IR_s}{R_p} \tag{10}$$

Substituting Equations (9) and (10) into Equation (8), the general formula from Kirchhoff's current law becomes:

$$I = I_{ph} - I_o \left[\exp\left(\frac{V + IR_s}{AV_T}\right) - 1\right] - \frac{V + IR_s}{R_p} \tag{11}$$

where:

$$V_T = \frac{N_S \times K \times T}{q}, \tag{12}$$

$$I_{ph} = \frac{G}{G_n}\left[I_{\text{pvn}} + K_1(T - T_n)\right], \tag{13}$$

$$I_0 = T_{0n}\left(\frac{T_n}{T}\right)^3 \exp\left[\frac{qE_g}{AK}\left(\frac{1}{T_n} - \frac{1}{T}\right)\right], \tag{14}$$

Substituting Equation (12) into Equation (11) and setting the resulting expression in the form $f(x) = 0$, gives:

$$f(x) = I_{ph} - I_o \left[\exp\left(\frac{V + IR_s}{AV_T}\right) - 1\right] - \frac{V + IR_s}{R_p} - I = 0 \tag{15}$$

where,

$$x = \begin{bmatrix} x_1 \\ x_2 \\ x_3 \\ x_4 \\ x_5 \end{bmatrix} = \begin{bmatrix} I_{ph} \\ I_0 \\ A \\ R_s \\ R_p \end{bmatrix} \tag{16}$$

Equation (15) is therefore a nonlinear equation with five variables which are the unknown parameters of the single diode PV module to be determined. Replacing the parameters by the x variables as in Equation (16) will give the equation below:

$$f_k(x) = x_1 - x_2 \left[\exp\left(\frac{V_k + I_k x_4}{x_3 V_T}\right) - 1\right] - \frac{V_k + I_k x_4}{x_5} - I_k = 0 \tag{17}$$

Substituting Equation (12) into Equation (17), we get

$$f_k(x) = x_1 - x_2 \left[e^{\frac{q(V_k + I_k x_4)}{N_S K T x_3}} - 1\right] - \frac{V_k + I_k x_4}{x_5} - I_k = 0 \tag{18}$$

where: I is cell current, I_{ph} is photo generated current, I_0 or I_D is diode reverse saturation current, q is electron elementary charge (1.602×10^{-19} coulombs), k is the Boltzmann constant (1.381×10^{-23} J/K), T is cell temperature, m is diode ideality factor, R_s is cell series resistance, R_{sh} or R_p is cell shunt resistance, and V is cell output voltage.

Let

$$\lambda = \frac{q}{KT} \tag{19}$$

Substituting Equation (19) into Equation (18) gives,

$$f_k(x) = x_1 - 10^{-6}x_2\left[e^{\frac{\lambda(V_k+I_kx_4)}{x_{3N_S}}} - 1\right] - \frac{V_k + I_kx_4}{x_5} - I_k = 0 \tag{20}$$

Since the single diode PV system has five parameters, we need five equations to solve for the unknown parameter. The equations are given by Equation (21):

$$\left.\begin{aligned} f_1(x) &= x_1 - 10^{-6}x_2\left[e^{\frac{\lambda(V_1+I_1x_4)}{x_{3N_S}}} - 1\right] - \frac{V_1 + I_1x_4}{x_5} - I_1 = 0 \\ f_2(x) &= x_1 - 10^{-6}x_2\left[e^{\frac{\lambda(V_1+I_1x_4)}{x_{3N_S}}} - 1\right] - \frac{V_1 + I_1x_4}{x_5} - I_2 = 0 \\ f_3(x) &= x_1 - 10^{-6}x_2\left[e^{\frac{\lambda(V_1+I_1x_4)}{x_{3N_S}}} - 1\right] - \frac{V_1 + I_1x_4}{x_5} - I_3 = 0 \\ f_4(x) &= x_1 - 10^{-6}x_2\left[e^{\frac{\lambda(V_1+I_1x_4)}{x_{3N_S}}} - 1\right] - \frac{V_1 + I_1x_4}{x_5} - I_4 = 0 \\ f_5(x) &= x_1 - 10^{-6}x_2\left[e^{\frac{\lambda(V_1+I_1x_4)}{x_{3N_S}}} - 1\right] - \frac{V_1 + I_1x_4}{x_5} - I_5 = 0 \end{aligned}\right\} \tag{21}$$

Equivalent nonlinear equations can be formulated for two and three-diode PV modules employing the same principles and procedures as those used for the single-diode PV system. However, it's important to note that the number of variables or parameters, and consequently the size of the resulting nonlinear system of equations, would increase with the number of diodes.

3.2. Methods of solution

The Newton-Raphson method is a reliable approach for finding approximate solutions or roots to numerical problems, particularly in cases where analytical methods prove impractical, especially for systems of nonlinear equations. However, it is crucial to note that if the initial guess is not in proximity to the solution or root, the Newton-Raphson method may fail to converge or converge to an incorrect root [16].

In the context of estimating parameters for photovoltaic (PV) modules, Newton's method has been widely employed by researchers to extract parameter values. Known for its ease of application and quadratic convergence [1,14], this method has been utilized in related studies to estimate five parameters of PV systems, employing carefully selected initial guess values [1]. In contrast, this study employs the Midpoint-Simpson-3/8 methods (MS-3/8), a quadrature rule, along with other existing methods to extract PV system parameters. The solutions obtained through these methods are then compared (refer to the studies of Ahmad et al. [17] and Bonkoungou et al. [18] for a detailed discussion of the methods).

4. Problem formulation

This investigation focused on estimating parameters for a single diode photovoltaic system, utilizing both secondary and primary data. The choice of secondary data was deliberate, as a different numerical method (specifically, the Newton-Raphson method) had been previously employed to address the same problem. Consequently, this study aimed to assess the newly developed solution methods introduced by the authors by applying them to the identical problem,

facilitating a comparison of results with those obtained through the Newton-Raphson method.

4.1. A PV module problem with secondary data

The issue with the secondary data was derived from a previously published article [15]. The mentioned article investigated a 40 W single-diode PV module with the following specifications, as shown in **Table 1** below.

Table 1. Specifications of a 40 W PV module.

Characteristics	**Specifications (value)**
Peak power (P_{mpp})	40 W
Voltage at peak power (V_{mpp})	16.6 V
Current at peak power (I_{mpp})	2.45 A
Short-circuit current (I_{sc})	2.8 A
Open-circuit voltage (V_{oc})	20.5 V
Number of cells (N_s)	36

In their 2017 study [15], presented two curves derived from experimental data, showcasing current and voltage values. The data were collected at various temperature and irradiance values, outlined as follows in **Table 2** below:

Table 2. Irradiation and temperature values for curves 1 & 2.

	Irradiation	**Temperature**
Curve 1	225 W/m^2	25 ℃
Curve 2	596.8 W/m^2	35 ℃

Current and voltage values were extracted from the two curves to formulate the system of nonlinear equations for the 40 W PV module. These extracted values served as the data used in the analysis and are summarized in **Tables 3** and **4**.

Table 3. Current and voltage values for curve 1.

$\boldsymbol{V_1, I_1}$	$\boldsymbol{V_2, I_2}$	$\boldsymbol{V_3, I_3}$	$\boldsymbol{V_4, I_4}$	$\boldsymbol{V_5, I_5}$
3.00, 0.62	8.00, 0.60	12.00, 0.56	17.00, 0.30	18.8, 0.02

Table 4. Current and voltage values for curve 2.

$\boldsymbol{V_1, I_1}$	$\boldsymbol{V_2, I_2}$	$\boldsymbol{V_3, I_3}$	$\boldsymbol{V_4, I_4}$	$\boldsymbol{V_5, I_5}$
3.00, 1.58	8.00, 1.54	12.5, 1.57	16.00, 0.4	19.5, 0.01

The system of nonlinear equations, illustrated by the single-diode model in Equation (22) below, is subsequently solved for the five parameters. This is achieved by employing the authors' proposed Broyden-like methods in conjunction with an existing numerical method (Newton-Raphson method). The results obtained from these methods are then compared for evaluation.

$$
\begin{aligned}
f_1(x) &= x_1 - 10^{-6}x_2\left(e^{\frac{\lambda(V_1+I_1x_4)}{36x_3}} - 1\right) - \frac{(V_1 + I_1x_4)}{x_5} - I_1 = 0 \\
f_2(x) &= x_1 - 10^{-6}x_2\left(e^{\frac{\lambda(V_2+I_2x_4)}{36x_3}} - 1\right) - \frac{(V_2 + I_2x_4)}{x_5} - I_2 = 0 \\
f_3(x) &= x_1 - 10^{-6}x_2\left(e^{\frac{\lambda(V_3+I_3x_4)}{36x_3}} - 1\right) - \frac{(V_3 + I_3x_4)}{x_5} - I_3 = 0 \\
f_4(x) &= x_1 - 10^{-6}x_2\left(e^{\frac{\lambda(V_4+I_4x_4)}{36x_3}} - 1\right) - \frac{(V_4 + I_4x_4)}{x_5} - I_4 = 0 \\
f_5(x) &= x_1 - 10^{-6}x_2\left(e^{\frac{\lambda(V_5+I_5x_4)}{36x_3}} - 1\right) - \frac{(V_5 + I_5x_4)}{x_5} - I_5 = 0
\end{aligned}
\tag{22}
$$

where $\begin{bmatrix} x_1 \\ x_2 \\ x_3 \\ x_4 \\ x_5 \end{bmatrix} = \begin{bmatrix} I_{ph} \\ I_0 \\ A \\ R_s \\ R_p \end{bmatrix}$, with the initial guesses (IG) below.

Table 5. Initial guesses.

Initial guess (IG)	**Initial guess values**
1°	*X*0 = [1.5; 0.5; 1.0; 0.5; 50]
2°	*X*0 = [2.0; 0.1; 1.0; 1.0; 100]
3°	*X*0 = [2.0; 1.0; 1.0; 1.0; 100]
4°	*X*0 = [2.0; 1.0; 1.0; 1.0; 50]
5°	*X*0 = [0.6; 2.5; 1.5; 2.0; 100]

For the purpose of this research, **Table 5** is a set of initial values for the five parameters under consideration. Having encapsulated the entire PV parameter estimation problem in a system of five nonlinear equations with five unknowns, numerical methods can be employed to derive the parameters [20]. In the instance of the Newton-Raphson method, its formula is expressed as follows:

$$
\begin{bmatrix} x_{1,n+1} \\ x_{2,n+1} \\ x_{3,n+1} \\ x_{4,n+1} \\ x_{5,n+1} \end{bmatrix} = \begin{bmatrix} x_{1,n} \\ x_{2,n} \\ x_{3,n} \\ x_{4,n} \\ x_{5,n} \end{bmatrix} - \begin{bmatrix} \frac{\partial f_1}{\partial x_1} & \frac{\partial f_1}{\partial x_2} & \frac{\partial f_1}{\partial x_3} & \frac{\partial f_1}{\partial x_4} & \frac{\partial f_1}{\partial x_5} \\ \frac{\partial f_2}{\partial x_1} & \frac{\partial f_2}{\partial x_2} & \frac{\partial f_2}{\partial x_3} & \frac{\partial f_2}{\partial x_4} & \frac{\partial f_2}{\partial x_5} \\ \frac{\partial f_3}{\partial x_1} & \frac{\partial f_3}{\partial x_2} & \frac{\partial f_3}{\partial x_3} & \frac{\partial f_3}{\partial x_4} & \frac{\partial f_3}{\partial x_5} \\ \frac{\partial f_4}{\partial x_1} & \frac{\partial f_4}{\partial x_2} & \frac{\partial f_4}{\partial x_3} & \frac{\partial f_4}{\partial x_4} & \frac{\partial f_4}{\partial x_5} \\ \frac{\partial f_5}{\partial x_1} & \frac{\partial f_5}{\partial x_2} & \frac{\partial f_5}{\partial x_3} & \frac{\partial f_5}{\partial x_4} & \frac{\partial f_5}{\partial x_5} \end{bmatrix}^{-1} \begin{bmatrix} f_1(x_n) \\ f_2(x_n) \\ f_3(x_n) \\ f_4(x_n) \\ f_5(x_n) \end{bmatrix}
\tag{23}
$$

The Jacobian matrix's general form for the PV system problem is crucial, as it dictates which numerical method demands a lower computational time for solution. In the Newton-Raphson method, the inverse Jacobian matrix is computed at each iterative step. Conversely, in the proposed method in this study, the values are updated only between successive iterative steps.

$$J^{-1}=\begin{bmatrix} 1 & 10^{-6}\left(e^{\frac{\lambda(V_1+I_1x_4)}{12x_3}}-1\right) & \frac{10^{-6}x_2(V_1+I_1x_4)\lambda e^{\frac{\lambda(V_1+I_1x_4)}{12x_3}}}{12x_3^2} & \frac{10^{-6}I_1x_2\lambda e^{\frac{\lambda(V_1+I_1x_4)}{12x_3}}}{12x_3^2}-\frac{I_1}{x_5} & \frac{V_1+I_1x_4}{x_5^2} \\ 1 & 10^{-6}\left(e^{\frac{\lambda(V_2+I_2x_4)}{12x_3}}-1\right) & \frac{10^{-6}x_2(V_2+I_2x_4)\lambda e^{\frac{\lambda(V_2+I_2x_4)}{12x_3}}}{12x_3^2} & \frac{10^{-6}I_2x_2\lambda e^{\frac{\lambda(V_2+I_2x_4)}{12x_3}}}{12x_3^2}-\frac{I_2}{x_5} & \frac{V_2+I_2x_4}{x_5^2} \\ 1 & 10^{-6}\left(e^{\frac{\lambda(V_3+I_3x_4)}{12x_3}}-1\right) & \frac{10^{-6}x_2(V_3+I_3x_4)\lambda e^{\frac{\lambda(V_3+I_3x_4)}{12x_3}}}{12x_3^2} & \frac{10^{-6}I_3x_2\lambda e^{\frac{\lambda(V_3+I_3x_4)}{12x_3}}}{12x_3^2}-\frac{I_3}{x_5} & \frac{V_3+I_3x_4}{x_5^2} \\ 1 & 10^{-6}\left(e^{\frac{\lambda(V_4+I_4x_4)}{12x_3}}-1\right) & \frac{10^{-6}x_2(V_4+I_4x_4)\lambda e^{\frac{\lambda(V_4+I_4x_4)}{12x_3}}}{12x_3^2} & \frac{10^{-6}I_4x_2\lambda e^{\frac{\lambda(V_4+I_4x_4)}{12x_3}}}{12x_3^2}-\frac{I_4}{x_5} & \frac{V_4+I_4x_4}{x_5^2} \\ 1 & 10^{-6}\left(e^{\frac{\lambda(V_5+I_5x_4)}{12x_3}}-1\right) & \frac{10^{-6}x_2(V_5+I_5x_4)\lambda e^{\frac{\lambda(V_5+I_5x_4)}{12x_3}}}{12x_3^2} & \frac{10^{-6}I_5x_2\lambda e^{\frac{\lambda(V_5+I_5x_4)}{12x_3}}}{12x_3^2}-\frac{I_5}{x_5} & \frac{V_5+I_5x_4}{x_5^2} \end{bmatrix} \quad (24)$$

4.2. The PV module problem with primary data

A crucial step in this research, crucial to simulating the proposed numerical methods, involved collecting experimental data from the photovoltaic system setup [19–21]. The study focused on a monocrystalline 10 W PV module with the following specifications in **Table 6** below:

Table 6. Mono crystalline 10 W PV module specification (STC: G = 1000 W/m^2 and T = 25 °C).

Characteristics	**Specifications (value)**
Peak power (P_{mpp})	10 W
Voltage at peak power (V_{mpp})	9 V
Current at peak power (I_{mpp})	0.8 A
Short-circuit current (I_{sc})	0.9 A
Open-circuit voltage (V_{oc})	10.4 V
Number of cells (N_s)	12

To facilitate the extraction of parameters from the modeled PV system using the proposed enhanced numerical methods, voltage-current characteristic curves were generated using data gathered under three distinct weather conditions. The practical experiment involved the following steps to obtain data:

Step one: Three tests were carried out using the same PV module but at different times of the day (i.e., morning, afternoon (sunny day), and cloudy day).

Step two: The data obtained was used to draw graphs indicating the relationships between current and voltage and voltage and power, as shown in as shown in **Figures 2–9** below.

Step three: Five data points corresponding to voltage and current from **Figures 4, 6** and **8** were selected. The selection was done with respect to the positioning of parameters on the standard voltage-current characteristic curve found in the literature, as shown in **Figures 2** and **3** below.

Step four: The data obtained above were then used together with the proposed numerical methods to extract and approximate the parameters of the modelled 10 W PV module.

Following the above steps, the 10 W PV system was set up on the campus of Regentropfen College of Applied Sciences (ReCAS), located in a community called Kansoe in the Bongo District of the Upper East Region, Ghana. Data values for current and voltage were picked at different times, starting in the morning, afternoon, and on a cloudy day. **Table 7** summarizes the data for different times of a day using 10W PV system.

Table 7. Data from 10 W photovoltaic system at different times of a day.

Morning			**Afternoon—Sunny day**			**Cloudy day**		
V	***I***	***P***	***V***	***I***	***P***	***V***	***I***	***P***
0.103	0.0064	0.0006592	0.18	0.131	0.02358	0.411	0.313	0.128643
0.105	0.1403	0.0147315	0.244	0.131	0.031964	0.842	0.281	0.236602
0.105	0.3151	0.0330855	0.526	0.131	0.068906	0.861	0.251	0.216111
0.105	0.6703	0.0703815	0.472	0.131	0.061832	0.897	0.256	0.229632
0.103	1.003	0.103309	0.649	0.131	0.085019	1.181	0.264	0.311784
0.102	1.504	0.153408	0.955	0.128	0.12224	1.6	0.254	0.4064
0.1	2.2492	0.22492	1.383	0.127	0.175641	2.127	0.232	0.493464
0.099	3.274	0.324126	2.216	0.127	0.281432	3.265	0.222	0.72483
0.098	4.919	0.482062	2.957	0.127	0.375539	4.58	0.225	1.0305
0.094	7.012	0.659128	4.41	0.129	0.56889	6.8	0.222	1.5096
0.078	8.5	0.663	7.15	0.122	0.8723	8.8	0.181	1.5928
0.026	9.539	0.248014	8.36	0.112	0.93632	9.14	0.15	1.371
			8.73	0.102	0.89046	9.29	0.137	1.27273
			8.9	0.095	0.8455	9.37	0.13	1.2181
			9.71	0.027	0.26217	9.62	0.127	1.22174
						9.73	0.126	1.22598
						9.6	0.121	1.1616
						9.982	0.059	0.588938

4.3. Typical PV module characteristic curve

From literature, the characteristic curve showing the relationship between voltage and current, and voltage and power, for a PV module is as shown in **Figures 2** and **3** respectively below.

Based on the curves presented above, it was anticipated that the graphs generated from the primary data acquired for the 10 W PV module in this study would exhibit similarities to **Figures 2** and **3** depicted earlier.

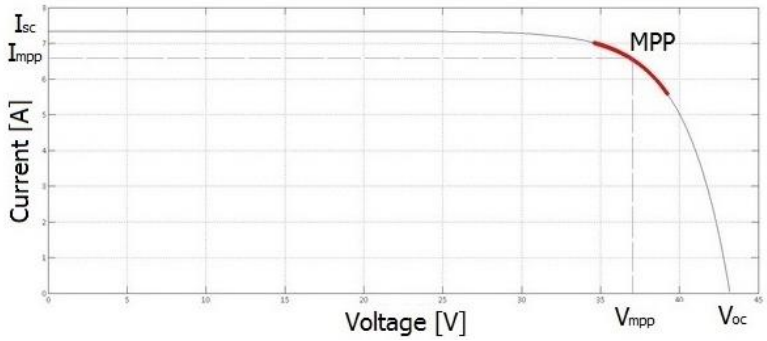

Figure 2. Standard voltage—Current characteristic curve from literature [9].

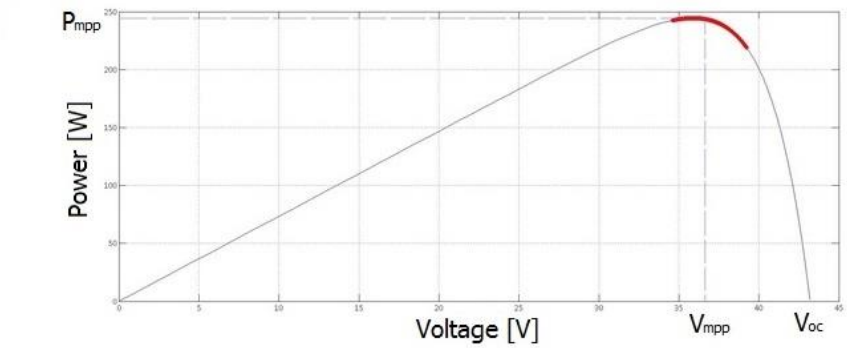

Figure 3. Standard voltage—Power characteristic curve from literature [9].

4.4. Experimental data output graphs for primary PV data

Figure 4 was generated by plotting the voltage and current values from **Table 8**, corresponding to the morning recordings. The resulting graph exhibited similar features to the standard PV module curve depicted in **Figure 2**.

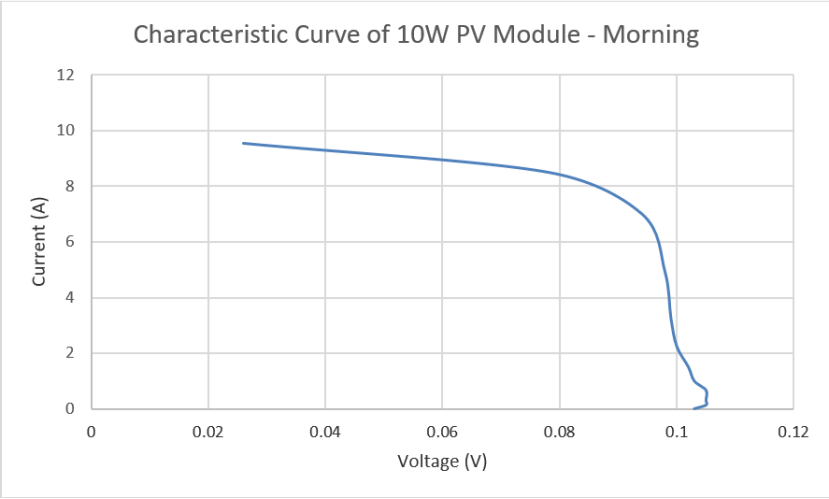

Figure 4. Relationship between voltage and current—Morning.

Table 8. Current and voltage values for morning.

V_1, I_1	V_2, I_2	V_3, I_3	V_4, I_4	V_5, I_5
0.026, 9.539	0.026, 9.500	0.075, 8.5	0.099, 3.274	0.105, 0.1403

Five voltage values, along with their corresponding current values, were chosen

from the graph to represent the morning conditions and are documented in **Table 8**. V_1, V_2, V_3, V_4, V_5 denote the voltage values, while I_1, I_2, I_3, I_4, I_5 represent the corresponding current values.

The morning values for voltage and power were also plotted to obtain the graph as shown in **Figure 5** below.

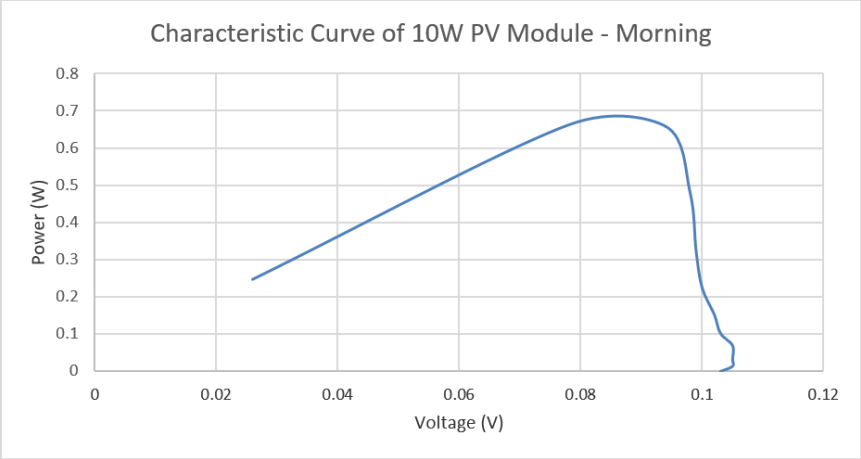

Figure 5. Relationship between voltage and power—Morning.

In a similar manner, values for current and voltage recorded on a sunny day (afternoon) were also plotted to obtain the **Figure 6**.

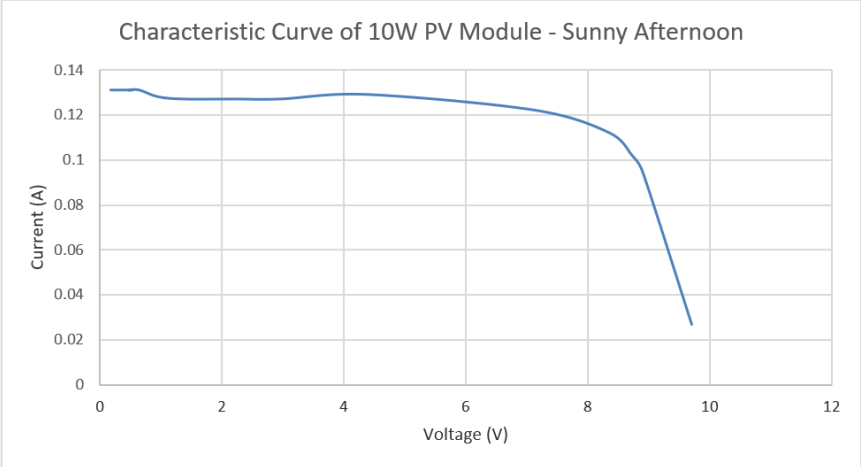

Figure 6. Relationship between voltage and current—Sunny day.

The **Table 9** are data representing current and voltage values for the sunny day and these values were selected from the graph.

Table 9. Current and voltage values for sunny day.

V_1, I_1	V_2, I_2	V_3, I_3	V_4, I_4	V_5, I_5
0.244, 0.131	4.41, 0.129	8.36, 0.112	8.9, 0.095	9.71, 0.027

The voltage and power values for sunny day were also plotted to obtain the **Figure 7**.

Another test was carried out on a cloudy day to obtain data for the current and

voltage of the 10 W PV module. Data for the current and voltage was plotted and represented in **Figure 8**.

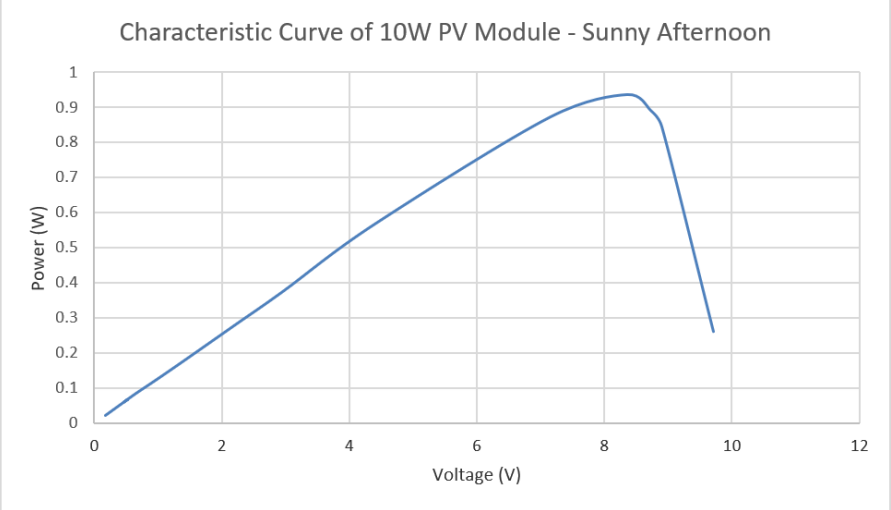

Figure 7. Relationship between voltage and power—Sunny day.

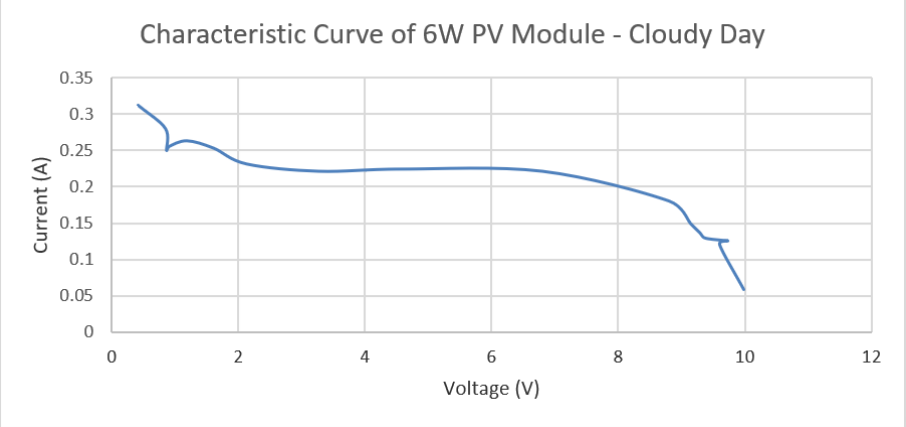

Figure 8. Relationship between voltage and current—Cloudy day.

The **Table 10** contains values of current and voltage selected from the data of cloudy day, for the computation of the parameters of the PV module.

Table 10. Current and voltage values for cloudy day.

V_1, I_1	V_2, I_2	V_3, I_3	V_4, I_4	V_5, I_5
0.411, 0.313	4.58, 0.225	8.8, 0.181	8.9, 0.095	9.37, 0.13

The graph in **Figure 9** is the voltage and power values for the cloudy day readings.

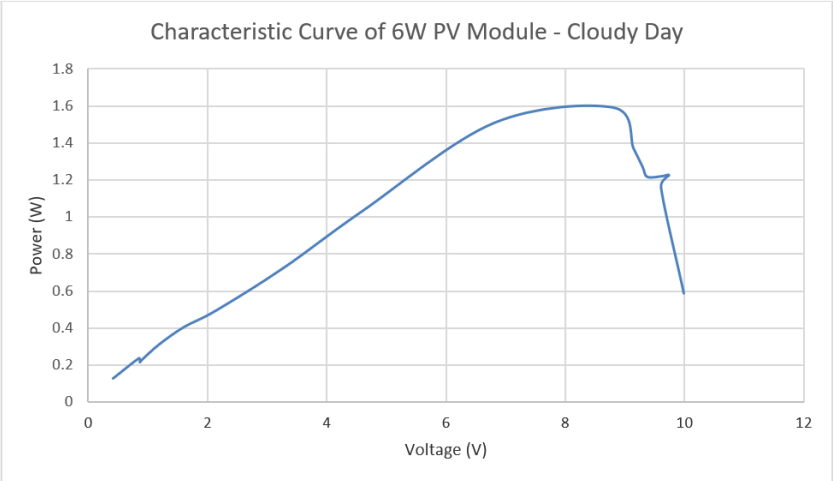

Figure 9. Relationship between voltage and power—Cloudy day.

Using the single-diode model, the photovoltaic system problem described above in Equation (22) is now written as Equation (25). Estimations of the parameters here are then carried out for the morning, sunny and cloudy days.

$$
\begin{aligned}
K=1&: f_1(x) = x_1 - 10^{-6}x_2\left[e^{\frac{\lambda(V_1+I_1x_4)}{12x_3}} - 1\right] - \frac{V_1+I_1x_4}{x_5} - I_1 = 0\\
K=2&: f_2(x) = x_1 - 10^{-6}x_2\left[e^{\frac{\lambda(V_2+I_2x_4)}{12x_3}} - 1\right] - \frac{V_2+I_2x_4}{x_5} - I_2 = 0\\
K=3&: f_3(x) = x_1 - 10^{-6}x_2\left[e^{\frac{\lambda(V_3+I_3x_4)}{12x_3}} - 1\right] - \frac{V_3+I_3x_4}{x_5} - I_3 = 0\\
K=4&: f_4(x) = x_1 - 10^{-6}x_2\left[e^{\frac{\lambda(V_4+I_4x_4)}{12x_3}} - 1\right] - \frac{V_4+I_4x_4}{x_5} - I_4 = 0\\
K=5&: f_5(x) = x_1 - 10^{-6}x_2\left[e^{\frac{\lambda(V_5+I_5x_4)}{12x_3}} - 1\right] - \frac{V_5+I_5x_4}{x_5} - I_5 = 0
\end{aligned}
\tag{25}
$$

5. Results and discussion for PV module problem with secondary data

The outcomes presented in **Table 11** illustrate the extracted parameters of the PV module problem, computed using both the Newton-Raphson method (NR) and the Midpoint-Simpson 3/8 method (MS-3/8). The results clearly demonstrate that both methods successfully converged to a solution across all five categories of initial guesses considered in this research.

While there were slight variations in the values of individual parameters in terms of decimal places, both methods yielded approximately the same result. This suggests that the MS-3/8 method is comparably effective. Ultimately, the results in **Table 11** establish that the MS-3/8 method is notably faster and more efficient than the Newton-Raphson method, as it required fewer iterations for all the initial guesses compared to the Newton-Raphson method. **Table 11** below summarizes the data obtained for curve 1.

Table 11. Obtained parameters for the curve 1.

IG	$x_1 = I_{ph}$			$x_2 = I_0$			$x_3 = A$			$x_4 = R_s$			$x_5 = R_p$			Number of iterations		
	NR	MS3/8	TS-3/8	NR	MS3/8	TS-3/8	NR	MS3/8	TS-3/8	NR	MS3/8	TS-3/8	NR	MS3/8	TS3/8	NR	MS8/8	TS3/8
1°	0.6687	0.6632	0.6612	0.2006	0.2000	0.2000	1.4288	1.4290	1.4290	1.1686	1.2002	1.2002	120.58	120.00	120.00	9	8	9
2°	0.6687	0.6632	0.6612	0.2006	0.2000	0.2000	1.4288	1.4290	1.4290	1.1686	1.2002	1.2002	120.58	120.00	120.00	7	4	6
3°	0.6687	0.6632	0.6612	0.2006	0.2000	0.2000	1.4288	1.4290	1.4290	1.1686	1.2002	1.2002	120.58	120.00	120.00	9	5	7
4°	0.6687	0.6632	0.6612	0.2006	0.2000	0.2000	1.4288	1.4290	1.4290	1.1686	1.2002	1.2002	120.58	120.00	120.00	9	5	6
5°	0.6687	0.6632	0.6612	0.2006	0.2000	0.2000	1.4288	1.4290	1.4290	1.1686	1.2002	1.2002	120.58	120.00	120.00	4	2	4

Similarly, the outcomes presented in **Table 12** reveal the parameter values of the PV module, computed using both the Newton-Raphson and Midpoint-Simpson 3/8 methods, utilizing certain current and voltage values from curve 2.

The results from **Table 12** affirm that both methods successfully converged for all the selected initial guess values. The parameter values obtained through both methods were approximately identical, with the MS-3/8 method demonstrating fewer iterations for all initial guesses compared to the Newton-Raphson method. This observation once again suggests that the MS-3/8 method is faster and more efficient than the Newton-Raphson method.

Table 12. Obtained parameters of the curve 2.

IG	$x_1 = I_{ph}$			$x_2 = I_0$			$x_3 = A$			$x_4 = R_s$			$x_5 = R_p$			Number of iterations		
	N	MS3/8	TS3/8	*N*	MS3/8	TS3/8	*N*	MS3/8	TS3/8	*N*	MS3/8	TS3/8	*N*	MS3/8	TS3/8	*N*	MS8/8	TS3/8
1°	1.8462	1.8500	1.8500	0.0441	0.0421	0.0421	1.0245	1.0311	1.0311	0.1979	0.2000	0.2000	58.92	59.00	59.00	5	2	3
2°	1.8462	1.8500	1.8500	0.0441	0.0421	0.0421	1.0245	1.0311	1.0311	0.1979	0.2000	0.2000	58.92	59.00	59.00	7	5	4
3°	1.8462	1.8500	1.8500	0.0441	0.0421	0.0421	1.0245	1.0311	1.0311	0.1979	0.2000	0.2000	58.92	59.00	59.00	8	4	5
4°	1.8462	1.8500	1.8500	0.0441	0.0421	0.0421	1.0245	1.0311	1.0311	0.1979	0.2000	0.2000	58.92	59.00	59.00	8	5	5
5°	1.8462	1.8500	1.8500	0.0441	0.0421	0.0421	1.0245	1.0311	1.0311	0.1979	0.2000	0.2000	58.92	59.00	59.00	4	3	4

Tables 11 and **12** showcase the current and voltage values derived from curves 1 and 2, which were utilized for estimating the parameters of the PV module through the Newton-Raphson and MS-3/8 methods. The successful execution of both methods indicates their efficiency in handling intricate nonlinear systems of equations, such as the PV module problem. Notably, the MS-3/8 method, with fewer iterations in both tables, emerges as the preferred method compared to Newton-Raphson for solving problems involving complex systems of nonlinear equations.

5.1. Results and discussion for PV module problem with primary data

Considering the complexities inherent in manually solving the photovoltaic system problem using the proposed methods, MATLAB codes were developed for the newly introduced methods (MS-3/8 and TS-3/8 methods). These codes were utilized to compute the parameters of the 10 W PV module. The computations were executed using MATLAB R2020b on a machine with the following specifications: CPU-AMD EI-2100APU with Radeon TM Graphics 1.00 GHz, installed memory (RAM)—4.00 GB, and system type—64-bit Operating System, X64-based processor. The program was designed to terminate when the number of iterations reached 500.

It is imperative to have approximate values in mind when applying the Newton-Raphson technique, MS-3/8, and TS-3/8 approaches, as these initial guesses should be in close proximity to the solution of the problem [15].

In the simulations conducted in this study, various guesses were employed, with some converging while others failed to converge. **Table 13** provides a summary of the initial guesses adopted for this study.

Table 13. Initial guesses.

Initial guess (IG)	Initial guess values
1°	$X0$ = [1.0; 2.0; 1.5; 1.0; 20]
2°	$X0$ = [1.0; 2.0; 1.5; 1.5; 20]
3°	$X0$ = [1.0; 1.5; 1.5; 1.5; 20]
4°	$X0$ = [1.0; 2.0; 1.0; 1.5; 20]
5°	$X0$ = [1.0; 1.5; 2.0; 2.0; 20]

Table 14 displays the results obtained when the MS-3/8 and TS-3/8 methods were applied to estimate the parameters of the 10 W PV module using morning data. Both methods generated solutions for all the initial guesses considered in the study. However, the individual values of the parameters exhibited slight variations between the two methods. This slight difference in parameter values for both methods could be attributed to the approximation of values within each method.

Upon closer examination of the values from both methods, it is evident that the MS-3/8 method consistently produced values greater than the TS-3/8 method, with an average difference of approximately 0.005 for all the initial guesses. Additionally, the results in **Table 14** highlight that the MS-3/8 method required fewer iterations to reach a solution compared to the TS-3/8 method, particularly for the current and voltage values obtained during the morning hours.

Table 14. Results of MS-3/8 and TS-3/8 methods—Morning.

IG	$x_1 = I_{ph}$		$x_2 = I_0$		$x_3 = A$		$x_4 = R_s$		$x_5 = R_p$		Number of iterations	
	MS3/8	TS3/8	MS3/8	TS3/8	MS3/8	TS3/8	MS3/8	TS3/8	MS3/8	TS3/8	MS3/8	TS8/8
1°	0.6522	0.6480	1.8420	1.8140	1.5325	1.4991	1.0421	1.0025	19.85	19.69	4	6
2°	0.6522	0.6480	1.8420	1.8140	1.5325	1.4991	1.0421	1.0025	19.85	19.69	4	5
3°	0.6522	0.6480	1.8420	1.8140	1.5325	1.4991	1.0421	1.0025	19.85	19.69	5	6
4°	0.6522	0.6480	1.8420	1.8140	1.5325	1.4991	1.0421	1.0025	19.85	19.69	4	7
5°	0.6522	0.6480	1.8420	1.8140	1.5325	1.4991	1.0421	1.0025	19.85	19.69	4	4

A test utilizing the data from a sunny day was conducted for both the MS-3/8 and TS-3/8 methods, and the summarized results are presented in **Table 15**. The data exhibited a consistent pattern of judgment when comparing the two methods. Both methods successfully converged for all the initial guesses employed in the study, and the parameter values obtained using the MS-3/8 method showed an average difference of 0.005 compared to the TS-3/8 method. Additionally, the MS-3/8 method required a lower number of iterations for all initial guesses considered compared to the TS-3/8 method.

Table 15. Results of MS-3/8 and TS-3/8 methods—Sunny day.

IG	$x_1 = I_{ph}$		$x_2 = I_0$		$x_3 = A$		$x_4 = R_s$		$x_5 = R_p$		Number of iterations	
	MS3/8	**TS3/8**	**MS3/8**	**TS3/8**	**MS3/8**	**TS3/8**	**MS3/8**	**TS3/8**	**MS3/8**	**TS3/8**	**MS3/8**	**TS8/8**
1°	0.4951	0.3992	1.5231	1.5001	1.3412	1.3315	0.9852	0.9431	19.69	19.60	3	6
2°	0.4951	0.3992	1.5231	1.5001	1.3412	1.3315	0.9852	0.9431	19.69	19.60	6	8
3°	0.4951	0.3992	1.5231	1.5001	1.3412	1.3315	0.9852	0.9431	19.69	19.60	4	6
4°	0.4951	0.3992	1.5231	1.5001	1.3412	1.3315	0.9852	0.9431	19.69	19.60	6	10
5°	0.4951	0.3992	1.5231	1.5001	1.3412	1.3315	0.9852	0.9431	19.69	19.60	3	5

To gain a comprehensive understanding of how these parameter values might vary under different weather conditions, data was extracted from the same setup on a cloudy day, and the outcomes were condensed in **Table 16** below. Both methods effectively estimated the parameters of the 10 W PV module in accordance with the specified initial guesses for the study. Consistent with the observations in **Tables 14** and **15**, data from **Table 16** indicated a lower number of iterations for the MS-3/8 method when compared to the TS-3/8 method.

Table 16. Results of MS-3/8 and TS-3/8 methods—Cloudy day.

IG	$x_1 = I_{ph}$		$x_2 = I_0$		$x_3 = A$		$x_4 = R_s$		$x_5 = R_p$		Number of iterations	
	MS3/8	**TS3/8**	**MS3/8**	**TS3/8**	**MS3/8**	**TS3/8**	**MS3/8**	**TS3/8**	**MS3/8**	**TS3/8**	**MS3/8**	**TS8/8**
1°	0.4410	0.4021	1.5420	1.5223	1.1213	1.1024	0.9827	0.9812	20.05	19.98	5	8
2°	0.4410	0.4021	1.5420	1.5223	1.1213	1.1024	0.9827	0.9812	20.05	19.98	4	6
3°	0.4410	0.4021	1.5420	1.5223	1.1213	1.1024	0.9827	0.9812	20.05	19.98	3	5
4°	0.4410	0.4021	1.5420	1.5223	1.1213	1.1024	0.9827	0.9812	20.05	19.98	4	6
5°	0.4410	0.4021	1.5420	1.5223	1.1213	1.1024	0.9827	0.9812	20.05	19.98	4	5

5.2. Mathematical model for four diodes PV module

In line with the research's third objective, which aims to introduce a mathematical model for a four-diode PV module, offering an innovative perspective to articulate and comprehend its characteristics and behavior within photovoltaic systems, **Figure 10** presents a proposed verification of the four-diode PV module model.

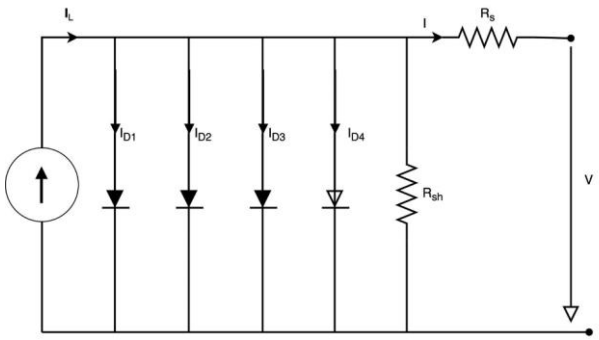

Figure 10. Electrical circuit of PV cell with four-diodes.

Applying Kirchhoff's current law to the above circuit diagram, we have

$$I = I_{ph} - I_{D1} - I_{D2} - I_{D3} - I_{D4} - I_{sh} \quad (26)$$

But

$$I_{D1} = I_{01}\left[\exp\left(\frac{V + IR_s}{A_1 \times V_T}\right) - 1\right] \tag{27}$$

$$I_{D2} = I_{02}\left[\exp\left(\frac{V + IR_s}{A_2 \times V_T}\right) - 1\right] \tag{28}$$

$$I_{D3} = I_{03}\left[\exp\left(\frac{V + IR_s}{A_3 \times V_T}\right) - 1\right] \tag{29}$$

$$I_{D4} = I_{04}\left[\exp\left(\frac{V + IR_s}{A_4 \times V_T}\right) - 1\right] \tag{30}$$

$$I_{sh} = \frac{V + IR_s}{R_p} \tag{31}$$

Hence

$$\begin{aligned} I = I_{ph} - I_{01}\left[\exp\left(\frac{V + IR_s}{A_1 \times V_T}\right) - 1\right] - I_{02}\left[\exp\left(\frac{V + IR_s}{A_2 \times V_T}\right) - 1\right] - I_{03}\left[\exp\left(\frac{V + IR_s}{A_3 \times V_T}\right) - 1\right] \\ - I_{04}\left[\exp\left(\frac{V + IR_s}{A_4 \times V_T}\right) - 1\right] - \frac{V + IR_s}{R_p} - I_k \end{aligned} \tag{32}$$

Set $f(x) = I$ and writing Equation (32) as $f(x) = 0$, we have

$$\begin{aligned} f(x) = I = I_{ph} - I_{01}\left[\exp\left(\frac{V + IR_s}{A_1 \times V_T}\right) - 1\right] - I_{02}\left[\exp\left(\frac{V + IR_s}{A_2 \times V_T}\right) - 1\right] - I_{03}\left[\exp\left(\frac{V + IR_s}{A_3 \times V_T}\right) - 1\right] \\ - I_{04}\left[\exp\left(\frac{V + IR_s}{A_4 \times V_T}\right) - 1\right] - \frac{V + IR_s}{R_p} - I_k \end{aligned} \tag{33}$$

Hence Equation (33) is a multidimensional function involving eleven parameters and eleven equations ($K = 1, 2, 3, \ldots, 11$). The parameters are as shown below:

$$\begin{bmatrix} x_1 \\ x_2 \\ x_3 \\ x_4 \\ x_5 \\ x_6 \\ x_7 \\ x_8 \\ x_9 \\ x_{10} \\ x_{11} \end{bmatrix} = \begin{bmatrix} I_{ph} \\ I_{01} \\ R_s \\ A_1 \\ I_{02} \\ A_2 \\ I_{03} \\ A_3 \\ I_{04} \\ A_4 \\ R_p \end{bmatrix}$$

Replacing the parameters in Equation (33) with their corresponding x variables above give:

$$\begin{aligned} f_k(x) = x_1 - x_2\left[\exp\left(\frac{V + Ix_3}{x_4 \times V_T}\right) - 1\right] - x_5\left[\exp\left(\frac{V + Ix_3}{x_6 \times V_T}\right) - 1\right] - x_7\left[\exp\left(\frac{V + Ix_3}{x_8 \times V_T}\right) - 1\right] \\ - x_9\left[\exp\left(\frac{V + Ix_3}{x_{10} \times V_T}\right) - 1\right] - \frac{V + Ix_3}{x_{11}} - I_k \end{aligned} \tag{34}$$

Substituting

$$V_T = \frac{N_S \times K \times T}{q}$$

Into Equation (34), we have

$$f_k(x) = x_1 - x_2\left[e^{\frac{q(V + I_k x_3)}{x_4 N_s KT}} - 1\right] - x_5\left[e^{\frac{q(V + I_k x_3)}{x_6 N_s KT}} - 1\right] - x_7\left[e^{\frac{q(V + I_k x_3)}{x_8 N_s KT}} - 1\right] - x_9\left[e^{\frac{q(V + I_k x_3)}{x_{10} N_s KT}} - 1\right] - \frac{V + Ix_3}{x_{11}} - I_k \tag{35}$$

Let $\lambda = \frac{q}{KT}$

$$f_k(x) = x_1 - x_2\left[e^{\frac{\lambda(V_3+I_3x_4)}{x_4N_S}} - 1\right] - x_5\left[e^{\frac{\lambda(V_3+I_3x_4)}{x_6N_S}} - 1\right] - x_7\left[e^{\frac{\lambda(V_3+I_3x_4)}{x_8N_S}} - 1\right] - x_9\left[e^{\frac{\lambda(V_3+I_3x_4)}{x_{10}N_S}} - 1\right] - \frac{V+Ix_3}{x_{11}} - I_k \quad (36)$$

For $K = 1, 2, 3, \ldots, 11$ we get the following system of nonlinear equations with eleven unknowns.

$$\begin{aligned}
f_1(x) &= x_1 - x_2\left[e^{\frac{\lambda(V_3+I_3x_4)}{x_4N_S}} - 1\right] - x_5\left[e^{\frac{\lambda(V_3+I_3x_4)}{x_6N_S}} - 1\right] - x_7\left[e^{\frac{\lambda(V_3+I_3x_4)}{x_8N_S}} - 1\right] - x_9\left[e^{\frac{\lambda(V_3+I_3x_4)}{x_{10}N_S}} - 1\right] - \frac{V+Ix_3}{x_{11}} - I_1 \\
f_2(x) &= x_1 - x_2\left[e^{\frac{\lambda(V_3+I_3x_4)}{x_4N_S}} - 1\right] - x_5\left[e^{\frac{\lambda(V_3+I_3x_4)}{x_6N_S}} - 1\right] - x_7\left[e^{\frac{\lambda(V_3+I_3x_4)}{x_8N_S}} - 1\right] - x_9\left[e^{\frac{\lambda(V_3+I_3x_4)}{x_{10}N_S}} - 1\right] - \frac{V+Ix_3}{x_{11}} - I_2 \\
f_3(x) &= x_1 - x_2\left[e^{\frac{\lambda(V_3+I_3x_4)}{x_4N_S}} - 1\right] - x_5\left[e^{\frac{\lambda(V_3+I_3x_4)}{x_6N_S}} - 1\right] - x_7\left[e^{\frac{\lambda(V_3+I_3x_4)}{x_8N_S}} - 1\right] - x_9\left[e^{\frac{\lambda(V_3+I_3x_4)}{x_{10}N_S}} - 1\right] - \frac{V+Ix_3}{x_{11}} - I_3 \\
f_4(x) &= x_1 - x_2\left[e^{\frac{\lambda(V_3+I_3x_4)}{x_4N_S}} - 1\right] - x_5\left[e^{\frac{\lambda(V_3+I_3x_4)}{x_6N_S}} - 1\right] - x_7\left[e^{\frac{\lambda(V_3+I_3x_4)}{x_8N_S}} - 1\right] - x_9\left[e^{\frac{\lambda(V_3+I_3x_4)}{x_{10}N_S}} - 1\right] - \frac{V+Ix_3}{x_{11}} - I_4 \\
f_5(x) &= x_1 - x_2\left[e^{\frac{\lambda(V_3+I_3x_4)}{x_4N_S}} - 1\right] - x_5\left[e^{\frac{\lambda(V_3+I_3x_4)}{x_6N_S}} - 1\right] - x_7\left[e^{\frac{\lambda(V_3+I_3x_4)}{x_8N_S}} - 1\right] - x_9\left[e^{\frac{\lambda(V_3+I_3x_4)}{x_{10}N_S}} - 1\right] - \frac{V+Ix_3}{x_{11}} - I_5 \\
f_6(x) &= x_1 - x_2\left[e^{\frac{\lambda(V_3+I_3x_4)}{x_4N_S}} - 1\right] - x_5\left[e^{\frac{\lambda(V_3+I_3x_4)}{x_6N_S}} - 1\right] - x_7\left[e^{\frac{\lambda(V_3+I_3x_4)}{x_8N_S}} - 1\right] - x_9\left[e^{\frac{\lambda(V_3+I_3x_4)}{x_{10}N_S}} - 1\right] - \frac{V+Ix_3}{x_{11}} - I_6 \quad (37) \\
f_7(x) &= x_1 - x_2\left[e^{\frac{\lambda(V_3+I_3x_4)}{x_4N_S}} - 1\right] - x_5\left[e^{\frac{\lambda(V_3+I_3x_4)}{x_6N_S}} - 1\right] - x_7\left[e^{\frac{\lambda(V_3+I_3x_4)}{x_8N_S}} - 1\right] - x_9\left[e^{\frac{\lambda(V_3+I_3x_4)}{x_{10}N_S}} - 1\right] - \frac{V+Ix_3}{x_{11}} - I_7 \\
f_8(x) &= x_1 - x_2\left[e^{\frac{\lambda(V_3+I_3x_4)}{x_4N_S}} - 1\right] - x_5\left[e^{\frac{\lambda(V_3+I_3x_4)}{x_6N_S}} - 1\right] - x_7\left[e^{\frac{\lambda(V_3+I_3x_4)}{x_8N_S}} - 1\right] - x_9\left[e^{\frac{\lambda(V_3+I_3x_4)}{x_{10}N_S}} - 1\right] - \frac{V+Ix_3}{x_{11}} - I_8 \\
f_9(x) &= x_1 - x_2\left[e^{\frac{\lambda(V_3+I_3x_4)}{x_4N_S}} - 1\right] - x_5\left[e^{\frac{\lambda(V_3+I_3x_4)}{x_6N_S}} - 1\right] - x_7\left[e^{\frac{\lambda(V_3+I_3x_4)}{x_8N_S}} - 1\right] - x_9\left[e^{\frac{\lambda(V_3+I_3x_4)}{x_{10}N_S}} - 1\right] - \frac{V+Ix_3}{x_{11}} - I_9 \\
f_{10}(x) &= x_1 - x_2\left[e^{\frac{\lambda(V_3+I_3x_4)}{x_4N_S}} - 1\right] - x_5\left[e^{\frac{\lambda(V_3+I_3x_4)}{x_6N_S}} - 1\right] - x_7\left[e^{\frac{\lambda(V_3+I_3x_4)}{x_8N_S}} - 1\right] - x_9\left[e^{\frac{\lambda(V_3+I_3x_4)}{x_{10}N_S}} - 1\right] - \frac{V+Ix_3}{x_{11}} - I_{10} \\
f_{11}(x) &= x_1 - x_2\left[e^{\frac{\lambda(V_3+I_3x_4)}{x_4N_S}} - 1\right] - x_5\left[e^{\frac{\lambda(V_3+I_3x_4)}{x_6N_S}} - 1\right] - x_7\left[e^{\frac{\lambda(V_3+I_3x_4)}{x_8N_S}} - 1\right] - x_9\left[e^{\frac{\lambda(V_3+I_3x_4)}{x_{10}N_S}} - 1\right] - \frac{V+Ix_3}{x_{11}} - I_{11}
\end{aligned}$$

Therefore, Equation (37) constitutes a set of nonlinear equations, serving as the model representation of a four-diode PV module that encompasses eleven equations and eleven unknown parameters.

6. Conclusion

This research initially focused on formulating mathematical models for estimating the parameters of the PV system, including single-diode, two-diode, three-diode, and four-diode PV system models. Testing these models using secondary data from a 40 W PV system and primary data from a 10 W PV system revealed their effectiveness with the Newton-Raphson method. However, when applying the MS-3/8 and TS-3/8 methods, a notable reduction in the number of iterations was observed, indicating that the MS-3/8 method is faster in estimating unknown parameters compared to the Newton-Raphson method.

Despite its complexity, the proposed four-diode model has the potential to provide more accurate parameter estimates for PV systems compared to single, double, and three-diode models. This is because related research has demonstrated that increasing the number of diodes can stabilize and enhance the accuracy of the model. However, a module with multiple diodes could be expensive to produce.

In conclusion, this research has presented compelling evidence to affirm that the

proposed methods (MS-3/8 and TS-3/8) are both efficient for solving systems of nonlinear equations. The MS-3/8 method, in particular, has demonstrated greater robustness, efficiency, and speed compared to the Newton-Raphson method. It is recommended for tackling complex problems, such as parameter estimation for a PV module.

Author contributions: Conceptualization, IA, BST and BS; methodology, IA, BST and BS; software, IA, BST and BS; validation, IA, BST and BS; formal analysis, IA, BST and BS; investigation, IA, BST and BS; resources, IA, BST and BS; data curation, IA, BST and BS; writing—original draft preparation, IA, BST and BS; writing—review and editing, IA; visualization, IA; supervision, BST and BS; project administration, IA; funding acquisition, IA. All authors have read and agreed to the published version of the manuscript.

Conflict of interest: The authors declare no conflict of interest.

References

1. Isaac A, Boakye Stephen T, Seidu B. A New Trapezoidal-Simpson 3/8 Method for Solving Systems of Nonlinear Equations. American Journal of Mathematical and Computer Modelling. 2021; 6(1): 1. doi: 10.11648/j.ajmcm.20210601.11
2. Hashim E, Talib Z. Study of the performance of five parameter model for monocrystalline silicon photovoltaic module using a reference data. FME Transactions. 2018; 46(4): 585-594. doi: 10.5937/fmet1804585t
3. Isaac A, Boakye Stephen T, Seidu B. A Comparison of Newly Developed Broyden-Like Methods for Solving System of Nonlinear Equations. International Journal of Systems Science and Applied Mathematics. 2021; 6(3): 77. doi: 10.11648/j.ijssam.20210603.11
4. Murakami T, Anbumozhi V. Global Situation of Small Modular Reactor Development and Deployment. ERIA; 2021.
5. Azure I. An Analysis of Solutions of Nonlinear Equations Using AI Inspired Mathematical Packages. International Journal of Systems Science and Applied Mathematics. Published online September 8, 2023. doi: 10.11648/j.ijssam.20230802.12
6. Reis LRD, Camacho RJ, Novacki DF. The Newton Raphson method in the extraction of parameters of the PV modules. In: Proceedings of the International Conference on Renewable Energies and Power Quality (ICREPQ' 17); Malaga, Spain. pp. 4-6.
7. Kheirkhah AR, Meschini Almeida CF, Kagan N, et al. Optimal Probabilistic Allocation of Photovoltaic Distributed Generation: Proposing a Scenario-Based Stochastic Programming Model. Energies. 2023; 16(21): 7261. doi: 10.3390/en16217261
8. Kheirkhah AR, Pozos AT, Zandrazavi SF, et al. A Stochastic Programming Model for the Optimal Allocation of Photovoltaic Distributed Generation in Electrical Distribution Systems Considering Load Variations and Generation Uncertainty. Simpósio Brasileiro de Sistemas Elétricos-SBSE. 2020; 1(1). doi: 10.48011/sbse.v1i1.2247
9. Pennsylvania State University. 2.6 The Hawthorne Effect. Advanced Energy Systems (AE 868). Available online: https://www.e-education.psu.edu/ae868/node/518 (accessed on 3 February 2021).
10. Prabu RT, Parasuraman S, Sahoo S, et al. The Numerical Algorithms and Optimization Approach Used in Extracting the Parameters of the Single-Diode and Double-Diode Photovoltaic (PV) Models. International Journal of Photoenergy. 2022; 2022: 1-9. doi: 10.1155/2022/5473266
11. Benabdelkrim B, Benatillah A. Modeling and Parameter Extraction of PV Cell Using Single- and Two-Diode Model. International Journal of Energetica. 2017; 2(2): 06. doi: 10.47238/ijeca.v2i2.40
12. Kisabo AB, Uchenna NC, Adebimpe FA. Newton's method for solving non-linear system of algebraic equations (NLSAEs) with MATLAB/Simulink and MAPLE. American Journal of Mathematical and Computer Modelling. 2017; 2(4): 117-131.
13. Belarbi M, Boudghene-Stambouli A, Belarbi EH, et al. A new algorithm of parameter estimation of a photovoltaic solar panel. Turkish Journal of Electrical Engineering & Computer Sciences. 2016; 24: 276-284. doi: 10.3906/elk-1308-60
14. Bikaneria J, Joshi SP, Joshi AR. Modeling and Simulation of PV Cell using One-diode model. International Journal of Scientific and Research Publications. 2013; 3(10): 1-4.

15. Sharadga H, Hajimirza S, Cari EPT. A Fast and Accurate Single-Diode Model for Photovoltaic Design. IEEE Journal of Emerging and Selected Topics in Power Electronics. 2021; 9(3): 3030-3043. doi: 10.1109/jestpe.2020.3016635
16. Dharmarajan R, Ramachandran R. PV Module Parameter Estimation Using Newton Raphson. International Research Journal of Multidisciplinary Technovation. 2019; 1(4), 28-40.
17. Ahmad T, Sobhan S, Nayan MdF. Comparative Analysis between Single Diode and Double Diode Model of PV Cell: Concentrate Different Parameters Effect on Its Efficiency. Journal of Power and Energy Engineering. 2016; 04(03): 31-46. doi: 10.4236/jpee.2016.43004
18. Bonkoungou D, Koalaga Z, Njomo D. Modelling and Simulation of photovoltaic module considering. International Journal of Emerging Technology and Advanced Engineering. 2013; 3(3): 493-502.
19. Rusirawan D, Farkas I. Identification of Model Parameters of the Photovoltaic Solar Cells. Energy Procedia. 2014; 57: 39-46. doi: 10.1016/j.egypro.2014.10.006
20. Pukhrem S. A Photovoltaic Panel Model in Matlab/Simulink. ResearchGate. 2013; 20-23.
21. Tamrakar V, Gupta SC, Sawle Y. Study of characteristics of single and double diode electrical equivalent circuit models of solar PV module. In: Proceedings of the 2015 International Conference on Energy Systems and Applications. doi: 10.1109/icesa.2015.7503362